Final report for the FK124527 project: Quantitative reconstruction of dNTP homeostatic networks

The evolution of the project and the resulting publications

As a preface, I would like to say that the project continuously deviated from the original plan as an adaptation to our acquired experience along the way. Nevertheless, I rate it as a success that we could turn the "nothing works out as planned" into several publications (cumulative IF 48) of which 2 high-profile ones related to two bioinformatics tools we developed: the nucleoTIDY software (http://nucleotidy.enzim.ttk.mta.hu/)(1) and the dNTPpoolDB database (https://dntppool.org/)(2). I indicated the changes in the yearly reports; however, I wish to briefly summarize the evolution of the project.

We started to reconstruct the kinetic model of the dNTP-producing metabolic network as planned, based on experimentally acquired kinetic parameters, metabolite, and enzyme concentrations (**Fig 1**). This dynamic model was intended to be used as a prediction tool for various treatments targeting dNTP metabolism. As *Mycobacteria* dispose of the most reduced set of dNTP metabolic enzymes and pathways, we started the reconstruction of the mycobacterial model. After having collected all the available data and constructed a model, however, we still had too many floating parameters which made the model non-functional.
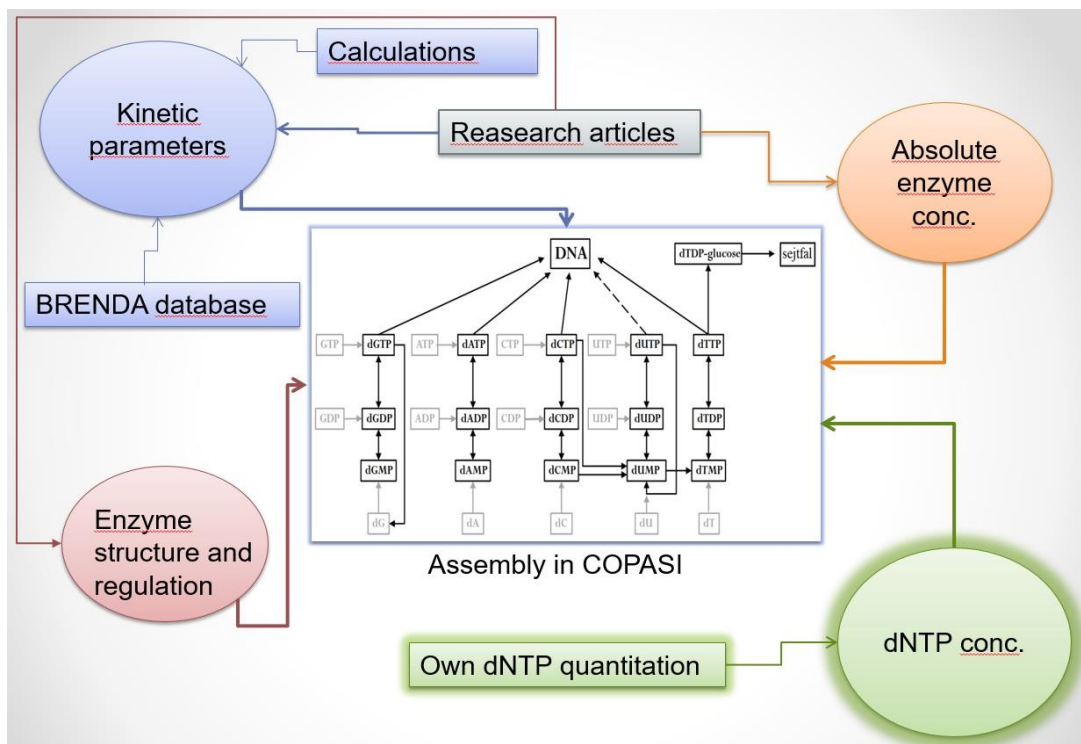

Figure 1 Principles of construction of the kinetic model of dNTP metabolism. We chose to break down all processes to basic differential equations which permitted to introduce regulation elements other than already set up in the software. Kinetic parameters were calculated from thermodynamic

ones when necessary, imposing thermodynamic constraints and setting binding processes fast enough not to be rate-limiting.

In parallel, we made efforts to determine the relevant enzyme concentrations in *Mycobacterium smegmatis* using mass spectrometry, as well as the dNTP concentrations using a fluorescent method. Neither of the two methods worked. We desperately needed a reliable dNTP quantitation method and therefore, we put much effort into developing one. At the same time, we decided to reconstruct the *Echerichia coli* (*E. coli*) dNTP metabolism model first even though it contains more enzymes than the mycobacterial system, as we found the highest number of available kinetic parameters for this species. Fortunately, the relevant enzyme concentrations in *E. coli* were also available in the literature (3). Therefore, we did not need to conduct otherwise complicated mass spectrometry experiments in collaboration. Meanwhile, we successfully measured dNTP concentrations in mycobacterial extracts using our new method and investigated aspects of dNTP metabolism within the cell (4). The extensive literature mining in the dNTP metabolism field brought about the idea of constructing a dNTPpool database. With the concentrated effort of all members of the team supplemented by two experts in database and webserver construction, we built a manually curated, critically evaluated and organized interactive database of the dNTP quantitation data accumulated in the literature for 50 years (2). Now we use this as a source for the validation of the kinetic model of dNTP metabolism we constructed, as well. The database contains the concentration changes of specific nucleotides in response to various treatments which we can use as an input in our model. We are now in the process of formulating the kinetic model paper which has been lagging for several reasons. One of which is that we wanted to use dNTP data we measure in *E. coli* under specific conditions to validate the model. However, these experiments were not reproducible. The late decision to abandon them and go with the database data instead also hindered the publication schedule. OTKA rules allow the joining of prospective publications to the final report of the grant later which is a good opportunity to get things straighten up at least in retrospect.

From now on, I will focus on the part of our results that is being published. Before we started the project, it had long been evident that a fine-tuned and well conserved concentration balance in the pool of deoxyribonucleoside 5'-triphosphates (deoxynucleotides or dNTPs) was necessary to maintain the normal cell cycle and the integrity of the genome. The pathways of dNTP metabolism have been researched for over 50 years, producing a large body of useful kinetic data. However, the last comprehensive quantitative model of dNTP metabolism was described in 1984 (5), well before the era of genome projects. Since then, a large number of important enzymes and regulation mechanisms have been discovered, and new central roles of dNTP pool homeostasis have been demonstrated in cancer development, ageing and viral infections (6,7). After thorough and lengthy literature mining and critical evaluation, we constructed a dynamic model of the dNTP producing metabolic pathways shown in **Fig 2**. Fundamental new aspects of our kinetic model are (*i*) the incorporation of dNTP metabolic enzyme abundance measured at the protein level, (*ii*) incorporation of critically assessed catalytic parameters of enzymes and drugs; (*iii*) measurement of cellular dNTP pools, and (*v*) validation based on our recently created dNTP pool database which contains the effects of modified enzyme variants and pharmacologically well-characterized drugs affecting dNTP metabolism (**Fig 1**).
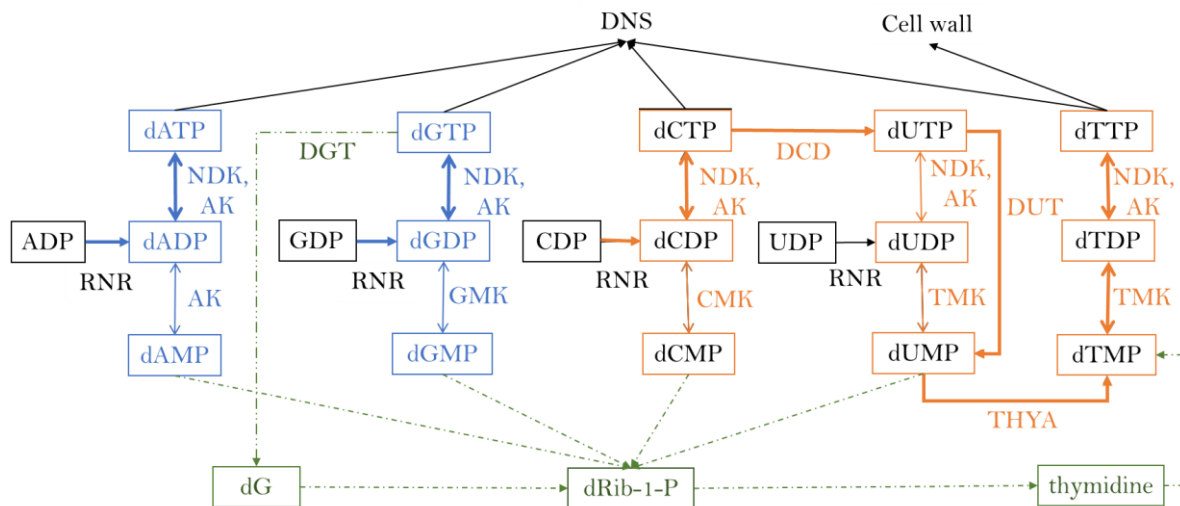
Figure 2 Metabolic pathways, enzymes and metabolites included in the model. The synthesis of nucleotides is a multistep regulated process which ensures optimal pools of nucleotides for genome and cell wall synthesis. We set the boundary of this network within the larger pyrimidine and purine synthetic network at the level of NDPs. NDP reduction by ribonucleotide reductase (RNR) is the entry to this dNTP producing network and generates dADP, dGTP, dCDP, and dUDP, the precursors for the corresponding dNTPs. In the cells, both the *de novo* (blue and red) and salvage pathways (green) are involved in the synthesis of dNTP. RNR, ribonucleotide reductase; NDK, nucleotide diphosphate kinase; AK, adenylate monophosphate kinase; GMK, guanine monophosphate kinase; CMK, cytidine monophosphate kinase; TMK, thymidine monophosphate kinase; DCD, dCTP deaminase; DUT, dUTPase; THYA, thymidylate synthase; DGT, dGTP triphosphohydrolase

Construction of the kinetic model

The dNTP synthesis system is a relatively well-defined part of the global cellular metabolism (8). It includes the purine synthetic pathways for dATP and dGTP productions and the pyrimidine synthetic pathways for dCTP, dUTP and dTTP. Although dUTP is not a canonical DNA building block, its synthesis is primary to the synthesis of dTTP (**Fig 2**) and its regulatory role has been demonstrated (9,10). Briefly, the input reaction of dNTP production is NDP reduction by the non-specific ribonucleotide reductase (RNR) which produces all dNDPs (**Fig 2**). These metabolites will then be processed by the also promiscuous nucleotide diphosphate kinase (NDK) to NTPs (11) (**Fig 2**). Additionally, monophosphate kinases are responsible for recycling the dNMPs to dNDPs (cytidine monophosphate kinase for dCMP – CMK; guanine monophosphate kinase for dGMP – GMK; thymidine monophosphate kinase for dTMP – TMK; and adenylate kinase for dAMP – AK) (**Fig 2**). Thymidylate is derived from either dCTP or dCMP. The deamination of dCTP by dCTP deaminase (DCD) generates dUTP, which is hydrolyzed by dUTP pyrophosphohydrolase (DUT) to dUMP, the substrate for the thymidylate synthase (ThyA) (**Fig 2**). The Dut reaction also prevents accumulation of mutagenic dUTP. In Gram-positive bacteria and eukaryotes, dCMP is deaminated directly to dUMP (12,13). Thymidylate synthase converts dUMP into dTMP, which is phosphorylated to dTDP by the action of thymidylate monophosphate kinase (TMK). dNTPs are used for the replication of DNA and DNA repair. dTTP is also a precursor for cell wall synthesis in bacteria (4,14). These are the outputs of the model.

Reconstruction of the mechanism of RNR

RNR is the best characterized enzyme of the process despite its complex structure and allosteric regulation. RNR accepts all bases, but the type of dNDP produced on the enzyme is dependent on the allosteric regulator (Ar) bound to the so-called specificity site. Also, the overall activity of the enzyme is dependent on the concentration ratio of dATP to ATP which bind to the activity site (15)(**Fig 3**). The type Ia RNR characteristic for *E. coli* and all eukaryotes consists of two subunits: subunit A and B, and structurally it is an A2B2 tetramer (16). The cellular concentration of subunit A and B are 2 and 1 µM respectively in unperturbed cells (3). In these low enzyme concentrations, subunit A is in a monomer (RNRA) – dimer (RNRA2) equilibrium while subunit B is a stable dimer (RNRB2)(17). The RNRA2 binds the allosteric regulator (Ar) nucleotides, which promote the assembly of the holoenzyme (17) (**Fig 3**). Interestingly, type Ib RNRs encoded by *Mycobacteria* and *Staphylococcus* species for example, lack this regulator induction mechanism and result in a different dNTP pool ratio (17). For the class Ia enzymes, the Michaelis-Menten constant (K_M) differs for each Ar and therefore, we introduced each of these parameters in the model in separate equations (Appendix). The active form of the RNR enzyme is the A2B2 tetramer while the ring-shaped A4B4 octamer is inactive (18) (**Fig 3**). dATP binding stabilizes the ocatemric form hence the inhibition of RNR activity by dATP (17,18). At physiological dATP concentrations, the *in vitro* RNR activity is practically zero (19). However, when ATP is also present at physiological concentration (~ 3 mM) there is an equilibrium between the active A2B2 and the inactive A4B4 forms (20).
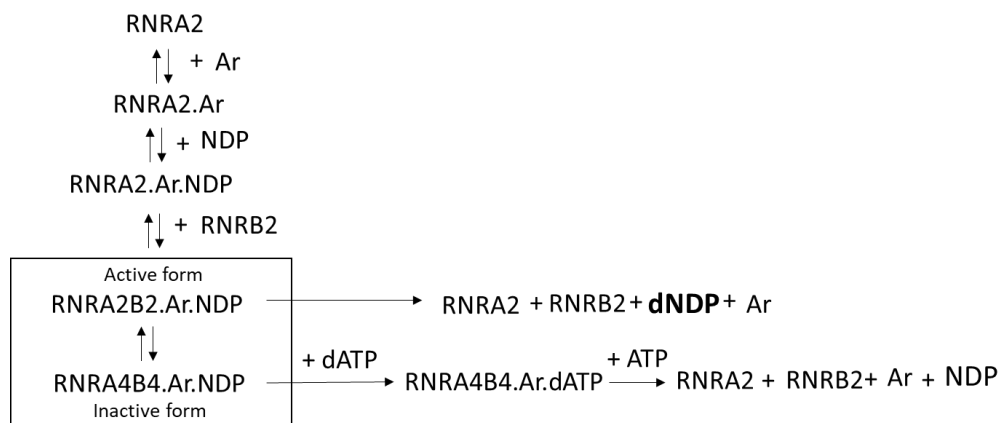

Figure 3 Elementary steps of the reactions catalyzed by RNR as formalized in the kinetic model. RNRA2, A subunit dimer; RNRB2, B subunit dimer; Ar, allosteric regulator

Reconstruction of the mechanism of NDK

dNDPs are further processed by (d)NDP kinase (NDK). NDK enzymes from various species show high sequence and crystal structure conservation and have identical active-site residues (21). Although there are some differences in their quaternary structures (most NDKs are hexameric while the *E. coli* and the yeast enzymes are tetrameric (22,23), the kinetic mechanism of NDKs is reported to be similar in each case. The enzyme follows a ping-pong bi-bi mechanism, where one product is released before the second substrate combines with the phosphorylated intermediate (21,24–26). There are no kinetic parameters available for the *E. coli* NDK. Based on the strong structural similarity, we used yeast (23,24) and mimivirus (27) kinetic parameters in the model (21,24,25). NDK readily binds all nucleotide-type metabolites including monophosphates and cAMP. However, these are unable to transfer phosphoryl groups and act as inhibitors (21). Our model contains NDK reactions including

only di- and triphosphates type substrates. The Michaelis constants for nucleotide triphosphates are about six times larger than those for nucleotide diphosphates, and the dead-end inhibition constants are one order of magnitude greater than the Michaelis constants, except for ADP (3-fold difference only). This suggests that ADP is a product, never a substrate and the reaction practically does not produce ATP (24). To simplify the model, we only included ATP as a phosphate donor to NDK even though all (d)NTPs can promote phosphoryl transfer. Due to the intracellular concentration conditions, ATP is practically the only quantitative phosphate donor. For the dead-end inhibition we only considered ATP and ADP as well. The local ATP:ADP ratio presumably is a strong regulator of the enzyme.
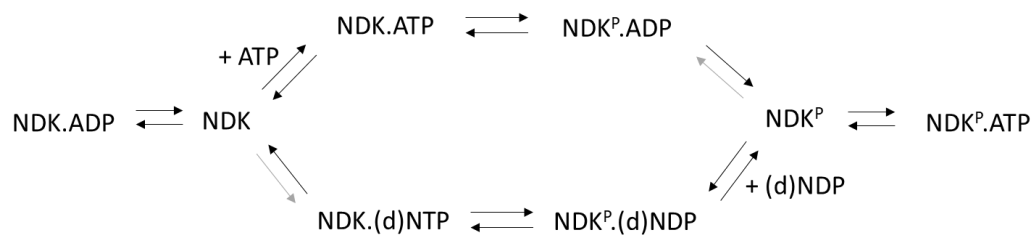

Figure 4 Elementary steps of the reactions catalyzed by NDK as formalized in the kinetic model. NDK action is represented as a ping-pong bi-bi mechanism with a stable phosphorylated enzyme intermediate. The function of the ping-pong mechanism is to redistribute metabolites according to their physiological concentrations. NDK has no preference for ribo- or deoxyribonucleotides or the phosphorylation state, every reaction is truly reversible.

Reconstruction of the mechanism of AK

The adenylate monophosphate kinase or adenylate kinase (AK) is an essential enzyme known to maintain the energy status of the cell by regulating the levels of ATP, ADP and AMP. By generating and distributing AMP metabolic signals, AK represents a unique hub within the cellular homeostatic network (28). We included it in our model as it was identified as an enzyme providing important NDK activity in *E. coli* (29,30).
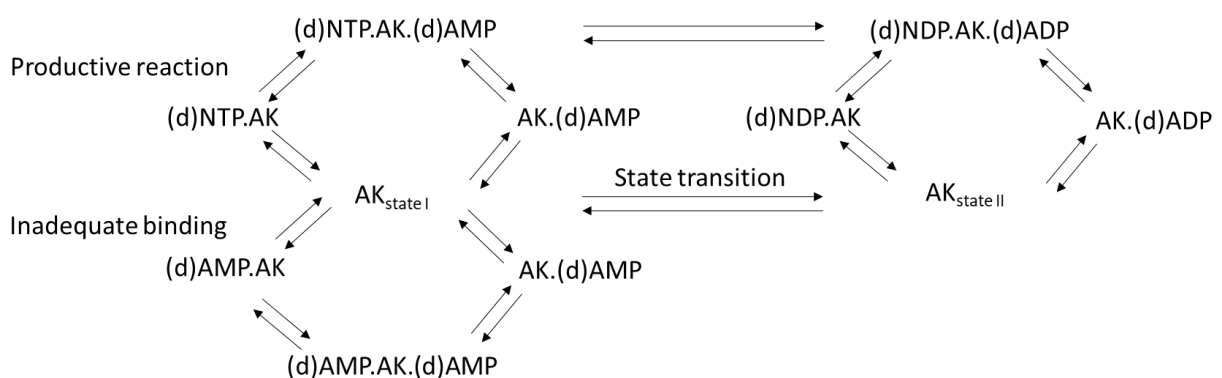
Figure 5 Elementary steps of the reactions catalyzed by AK as formalized in the kinetic model.

Experiments revealed that the AK generated dNTP from dNDP using ADP as phosphate donor (31). Structural studies suggested that out of the two binding sites, the AMP binding site requires at least five specific interactions with the nucleobase in contrast to a single interaction in the other site (ATP binding site), indicating that any NDP/dNDP might attach to the second site to be subsequently

phosphorylated (32). Before the inclusion of the NDK activity of the AK, the model could not reproduce experimentally measured dNTP pools.

The formalization of thymidylate synthesis

Thymidylate is *de novo* synthesized from dUMP by thymidylate synthase (ThyA) (**Fig 2**). dUMP is generated via various routes depending on the organism. In *E. coli*, there are two separate ways to produce dUMP. dCTP deaminase (DCD) transforms dCTP to dUTP, which is further broken down to dUMP by dUTPase (DUT). This pathway provides 70–80% of the total dUMP (33). The rest is produced through the reduction of UDP to dUDP which is phosphorylated to dUTP and then broken down by DUT.

DCD can bind dCTP, dUTP and dTTP at the same binding site with slight differences in their interaction network with the protein. Although the enzymes bind dUTP, there is no indication that the dUTP -> dCTP reaction happens physiologically (33,34). dTTP was shown to inhibit by stabilizing the inactive form of the enzyme (34) (**Fig 6**). Furthermore, increasing concentrations of dCTP increase the cooperativity of dTTP inhibition. In the model, we implemented all this information via a highly simplified manner. dTTP stabilizes the inactive form, while dCTP and dUTP are competitive inhibitors binding to the same active site (**Fig 6**). Few kinetic parameters are available for the *E. coli* DCD enzyme. We could use available inhibition parameters and set up the other kinetic parameters comparing experimental data available in the dNTP database (mainly on DCD mutants) with rounds of simulations.

DCD $\rightleftarrows$ InactDCD $\rightleftarrows$ InactDCD.dTTP

+ dCTP$\uparrow\downarrow$ + dTTP

DCD.dCTP $\longrightarrow$ DCD + dUTP
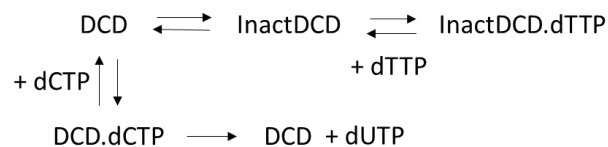
Figure 6 Elementary steps of the reactions catalyzed by DCD as formalized in the kinetic model

DUT is the enzyme that breaks down dUTP to dUMP. The incorporation of its enzymatic reaction into the model was straightforward as it is simple, and we have had extensive experience working with this enzyme (**Fig 7**).

+ dUTP

DUT $\rightleftarrows$ DUT.dUTP $\longrightarrow$ DUT + dUMP

Figure 7 Elementary steps of the reactions catalyzed by DUT as formalized in the kinetic model

ThyA is an essential enzyme for the *de novo* synthesis of dTMP, precursor for dTTP. The enzyme is a medically important one as it is considered a potential antimicrobial and anticancer drug target which is kinetically and structurally well studied (35). The methyltetrahydrofolate (mTHF) cofactor serves as both the one-carbon donor to the substrate dUMP and, subsequently, as reducing agent (35–37). In the model, the enzyme mechanism is implemented with the reported ordered BiBi mechanism, where the dUMP is the first substrate to bind followed by the binding of the cofactor (38) (**Fig 8**).

$$\text{ThyA} \underset{}{\overset{+ \text{ dUMP}}{\rightleftarrows}} \text{ThyA.dUMP} \underset{}{\overset{+ \text{ mTHF}}{\rightleftarrows}} \text{ThyA.dUMP.mTHF} \longrightarrow \text{ThyA} + \text{dTMP}$$

Figure 8 Elementary steps of the reactions catalyzed by ThyA as formalized in the kinetic model

Thymidylate kinase or thymidylate monophosphate kinase (TMK) is the essential enzyme catalyzing the reversible reaction of dTMP phosphorylation to produce dTDP using ATP as the main phosphate donor (38–40). Nevertheless, dATP is nearly as effective as ATP (38). It is the last specific enzyme in dTTP synthesis before the dTDP -> dTTP reaction which is catalyzed by the non-specific NDK. dUMP seems to be a competitive inhibitor for *E. coli* TMK and dTTP has a slight inhibitory effect (38). While the enzyme is essential, a mutant strain was created on complex genetic background having 4% residual TMK activity and fivefold higher K_M than that of the native enzyme. In this mutant, the concentration of dTMP was elevated as expected but without any significant change in the concentration of dTDP or dTTP (41). This suggests that TMK regulation is not sufficiently described. While TMK can process dUMP in addition to dTMP, the efficiency of the reaction is very low, and the K_M of the binding is around 2.5 mM, much higher than for dTMP. Other than that, dUMP phosphorylating enzymes are not known. The implementation of the kinetic mechanism of TMK and all other specific monophosphate kinases (**Fig 2**) is shown in **Fig 9**.
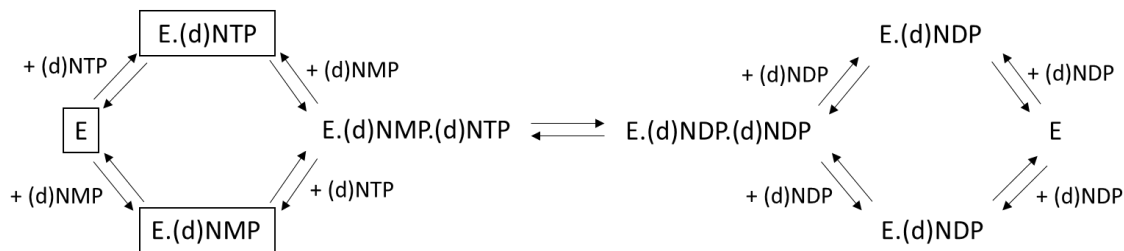
Figure 9 Elementary steps of the reactions catalyzed by nucleoside monophosphate kinases TMK, CMK and GMK as formalized in the kinetic model

Methods

For kinetic modelling, we used the COPASI software (https://copasi.org/). The enzyme reactions and their regulation are introduced as elementary reactions (see Appendix). Technical output is mainly done as time courses in which dNTP concentration changes are followed in time upon variation of a chosen parameter.

Experimentally measured kinetic parameters were retrieved from original articles and from the Brenda database (brenda-enzymes.org). Michaelis-Menten konstants (K_M), specific activities and turnover numbers are readily available, rate constants for elementary reactions (k_{on} and k_{off}) are scarcer. When necessary, k_{on} and k_{off} values were calculated from K_M using the equation

$$KM = \frac{koff + kcat}{kon}$$

The k_{on} is set to 10^5 µM^{-1}*s^{-1} for diffusion control (42). k_{cat} was neglected when it was much lower than k_{off}. For some reversible reactions, the revers k_{cat} parameters were unavailable. In these instances, we calculated k_{rev} from the global equilibrium constant (K') of the enzyme reactions retrieved from the Enyzme Thermodynamic Database (nist.gov) using the equation:

$$K' = \frac{1}{KmB} * \frac{1}{KmA} * KmC * KmD * \frac{k2}{k1}$$

As not all the necessary kinetic parameters were available for *E. coli,* the missing ones were approximated based on similar enzymes of different organisms. Enzyme concentrations were retrieved form (3). Metabolite concentrations were extracted from the BioNumbers database and from our own dNTP database (2,43). All parameters used in the model are included in the Appendix.

Major findings

Reproduction of reported dNTP pool balances in an isolated system

As a result of tedious optimization of kinetic parameters and regulation mechanisms, the *E. coli* kinetic model reproduces the quasi steady-state dNTP pools measured in bacterial cell lysates. This is quite remarkable considering that the model includes 149 elementary reactions and that many of the parameters of these reactions had to be approximated. We could also reproduce the directions and orders of magnitudes in dNTP pool changes reported upon genetic modification of the nucleotide metabolizing enzymes included in our model. During the recurrent optimization processes, we also revealed the robustness of various elements of this isolated metabolic network.

The coupling of enzyme cycles is crucial to support DNA polymerization

If our network is not isolated and we allow outward dNTP fluxes based on the calculation of the amount of dNTP incorporated into the newly synthesized DNA and into the cell wall under real cell growth conditions, the system is quickly depleted. After a few seconds, no dNTP remains. However, when the real-life outward flux is removed, the model can reproduce the measured dNTP pools as mentioned above. To produce enough dNTP that sufficiently supports DNA polymerization, we need to highly increase the rate constants of the chemical steps on the dNTP synthesizing enzymes (especially that of RNR) and/or highly increase the concentrations of the metabolic intermediates. In other terms, the sum of enzyme activities measured using separate purified enzymes and cytosolic metabolite concentrations do not sustain the need for dNTPs necessary for normal cell division. This deviation quantitatively explains for the first time the observations that dNTP synthesis enzymes are aggregated into complexes and to the sites of DNA polymerization. The bacterial NDK was shown to be an integral part of the dNTP synthetase machinery of the T4 phage (44). *In vitro* interactions of *E. coli* NDK with T4-encoded DNA polymerase, topoisomerase, RNR, TMK, DCD-DUT, and dihydro-folate reductase were demonstrated (30,45–48). It was shown early on that a multienzyme organization may give rise to efficient and rapid channeling of substrates between enzymes. The kinetic coupling between thymidylate synthesis enzymes isolated in a preorganized multienzyme complex was demonstrated (49). More recently, the assembly of thymidylate synthesis enzymes and their recruitment to the replication site was also demonstrated in human cells (50). In plants, the NDK interactome revealed a high number of nucleotide-dependent proteins as well (51). All evidence

suggests that DNA replication centers are fueled by a localized dNTP pool that is replenished much more rapidly without coming into equilibrium with the rest of the cellular pool. In our study, we show that experimentally measured cellular dNTP pools and the known enzyme mechanisms do not support the physiological DNA replication speed and therefore, coupling of the catalytic cycles between RNR, NDK and the thymidylate synthase enzymes is necessary.

Regulation of RNR determines the balance of the species-specific dNTP pool

During the kinetic simulations, we realized that relatively small changes in the allosteric regulation of RNR by various dNTPs may cause a characteristic change in the dNTP pool balance. At the same time, from our growing number of dNTP pool measurements in various species (**Fig 10**), we realized that i) the dNTP pool balance is markedly different in the different species, ii) similar pools coincide with similar RNR types acting in those species. Using these data and the information on the type of RNRs in these organisms we can relate the two phenomena and predict, based on genomic information, the dNTP constitution of an organism.
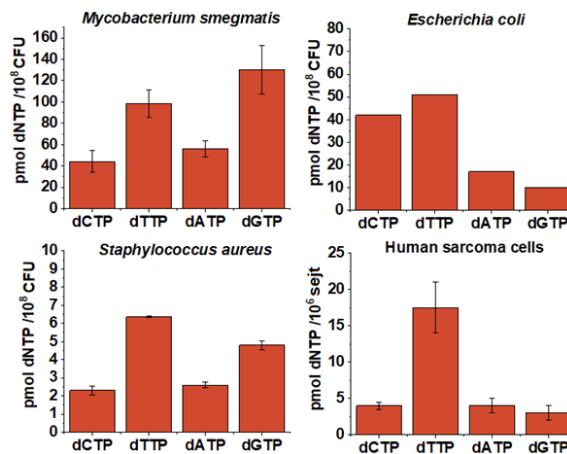
Figure 10 dNTP pool composition in various species. *Mycobacteria* encode class Ib and class II (not essential) RNR isoforms (52), *Staphylococcus* species encode class Ib and class III (anaerobic conditions only) RNR isoforms (53), while *E. coli* and humans encode class Ia RNR isoforms.

References

1.   Szabó JE, Surányi ÉV, Mébold B, Trombitás T, Cserepes M, Tóth J. A user-friendly, high-throughput tool for the precise quantitation of deoxyribonucleoside triphosphates from biological samples. Nucleic Acids Res. 2020;1:1–17.

2.   Pancsa R, Fichó E, Molnár D, Surányi ÉV, Trombitás T, Füzesi D, et al. dNTPpoolDB: a manually curated database of experimentally determined dNTP pools and pool changes in biological samples. Nucleic Acids Res [Internet]. 2022 Jan 7 [cited 2022 Aug 11];50(D1):D1508–14. Available from: https://pubmed.ncbi.nlm.nih.gov/34643700/

3.   Schmidt A, Kochanowski K, Vedelaar S, Ahrné E, Volkmer B, Callipo L, et al. The quantitative and condition-dependent Escherichia coli proteome. Nat Biotechnol 2015 341 [Internet]. 2016 Jan 1 [cited 2022 Aug 11];34(1):104–10. Available from: https://www.nature.com/articles/nbt.3418

4.   Hirmondó R, Horváth Á, Molnár D, Török G, Nguyen L, Tóth J. The effects of mycobacterial RmlA perturbation on cellular dNTP pool, cell morphology, and replication stress in Mycobacterium smegmatis. PLoS One [Internet]. 2022 Feb 1 [cited 2022 Aug 11];17(2). Available from: https://pubmed.ncbi.nlm.nih.gov/35202428/

5.   Jackson RC. A kinetic model of regulation of the deoxyribonucleoside triphosphate pool composition. Pharmacol Ther [Internet]. 1984 [cited 2017 Feb 19];24(2):279–301. Available from: http://www.ncbi.nlm.nih.gov/pubmed/6379685

6.   Mathews CK. Deoxyribonucleotide metabolism, mutagenesis and cancer. Nat Rev Cancer [Internet]. 2015 Aug 24 [cited 2017 Feb 18];15(9):528–39. Available from: http://www.ncbi.nlm.nih.gov/pubmed/26299592

7.   Stillman B. Deoxynucleoside triphosphate (dNTP) synthesis and destruction regulate the replication of both cell and virus genomes. Proc Natl Acad Sci [Internet]. 2013 Aug 27 [cited 2017 Feb 19];110(35):14120–1. Available from: http://www.ncbi.nlm.nih.gov/pubmed/23946423

8.   Rudd SG, Valerie NCK, Helleday T. Pathways controlling dNTP pools to maintain genome stability. DNA Repair. 2016.

9.   Tormo-Mas MA, Mir I, Shrestha A, Tallent SM, Campoy S, Lasa I, et al. Moonlighting bacteriophage proteins derepress staphylococcal pathogenicity islands. Nature [Internet]. 2010/05/18. 2010 Jun 10 [cited 2015 Feb 16];465(7299):779–82. Available from: http://www.pubmedcentral.nih.gov/articlerender.fcgi?artid=3518041&tool=pmcentrez&rendertype=abstract

10.   Szabó JE, Németh V, Papp-Kádár V, Nyíri K, Leveles I, Bendes AÁ, et al. Highly potent dUTPase inhibition by a bacterial repressor protein reveals a novel mechanism for gene expression control. Nucleic Acids Res [Internet]. 2014 Oct 29 [cited 2015 Jan 15];42(19):11912–20. Available from: http://nar.oxfordjournals.org/content/42/19/11912.long

11.   Mathews CK. Deoxyribonucleotides as genetic and metabolic regulators. FASEB J. 2014 Jun;1–9.

12.   MALEY GF, MALEY F. Nucleotide interconversions in embryonic and neoplastic tissues. I. The conversion of deoxycytidylic acid to deoxyuridylic acid and thymidylic acid. J Biol Chem [Internet]. 1959 Nov [cited 2022 Aug 20];234:2975–80. Available from: https://pubmed.ncbi.nlm.nih.gov/14420287/

13.   Hou HF, Liang YH, Li LF, Su XD, Dong YH. Crystal structures of Streptococcus mutans 2'-deoxycytidylate deaminase and its complex with substrate analog and allosteric regulator dCTP x Mg2+. J Mol Biol. 2008;377:220–31.

14.   Alphey MS, Pirrie L, Torrie LS, Boulkeroua WA, Gardiner M, Sarkar A, et al. Allosteric Competitive Inhibitors of the Glucose-1-phosphate Thymidylyltransferase

(RmlA) from *Pseudomonas aeruginosa*. ACS Chem Biol [Internet]. 2013 Feb 15 [cited 2018 Feb 1];8(2):387–96. Available from: http://www.ncbi.nlm.nih.gov/pubmed/23138692

15. Nordlund P, Reichard P. Ribonucleotide reductases. Annu Rev Biochem. 2006 Jan;75:681–706.

16. Ruskoski TB, Boal AK. The periodic table of ribonucleotide reductases. J Biol Chem [Internet]. 2021 Oct 1 [cited 2021 Oct 27];297(4):101137–8. Available from: http://www.jbc.org/article/S0021925821009388/fulltext

17. Crona M, Moffatt C, Friedrich NC, Hofer A, Sjöberg BM, Edgell DR. Assembly of a fragmented ribonucleotide reductase by protein interaction domains derived from a mobile genetic element. Nucleic Acids Res [Internet]. 2011 Mar [cited 2022 Aug 20];39(4):1381–9. Available from: https://pubmed.ncbi.nlm.nih.gov/20972217/

18. Greene BL, Nocera DG, Stubbe JA. Basis of dATP inhibition of RNRs. J Biol Chem [Internet]. 2018 Jun 29 [cited 2022 Aug 20];293(26):10413–4. Available from: https://pubmed.ncbi.nlm.nih.gov/29959279/

19. Fairman JW, Wijerathna SR, Ahmad MF, Xu H, Nakano R, Jha S, et al. Structural basis for allosteric regulation of human ribonucleotide reductase by nucleotide-induced oligomerization. Nat Struct Mol Biol. 2011 Mar;18(3):316–22.

20. Yang-Ting Chen P, Funk MA, Brignole EJ, Drennan CL. Disruption of an oligomeric interface prevents allosteric inhibition of Escherichia coli class Ia ribonucleotide reductase. J Biol Chem [Internet]. 2018 Jun 29 [cited 2022 Aug 21];293(26):10404–12. Available from: https://pubmed.ncbi.nlm.nih.gov/29700111/

21. Lascu I, Gonin P. The catalytic mechanism of nucleoside diphosphate kinases. J Bioenerg Biomembr [Internet]. 2000 [cited 2022 Aug 21];32(3):237–46. Available from: https://pubmed.ncbi.nlm.nih.gov/11768307/

22. Almaula N, Lu Q, Delgado J, Belkin S, Inouye M. Nucleoside diphosphate kinase from Escherichia coli. J Bacteriol [Internet]. 1995 [cited 2022 Aug 21];177(9):2524–9. Available from: https://pubmed.ncbi.nlm.nih.gov/7730286/

23. Jong AY, Ma JJ. Saccharomyces cerevisiae nucleoside-diphosphate kinase: purification, characterization, and substrate specificity. Arch Biochem Biophys [Internet]. 1991 [cited 2022 Aug 21];291(2):241–6. Available from: https://pubmed.ncbi.nlm.nih.gov/1659321/

24. Garces E, Cleland WW. Kinetic studies of yeast nucleoside diphosphate kinase. Biochemistry [Internet]. 1969 Feb 1 [cited 2022 Aug 21];8(2):633–40. Available from: https://pubmed.ncbi.nlm.nih.gov/5793714/

25. Mourad N, Parks RE. Erythrocytic nucleoside diphosphokinase. II. Isolation and kinetics. J Biol Chem. 1966 Jan 25;241(2):271–8.

26. Edlund B, Rask L, Olsson P, Wålinder O, Zetterqvist, Engström L. Preparation of crystalline nucleoside diphosphate kinase from baker's yeast and identification of 1-[32P]phosphohistidine as the main phosphorylated product of an alkaline hydrolysate of enzyme incubated with adenosine [32P]triphosphate. Eur J Biochem [Internet]. 1969 [cited 2022 Aug 21];9(4):451–5. Available from:

https://pubmed.ncbi.nlm.nih.gov/5806496/

27.   Jeudy S, Claverie JM, Abergel C. The nucleoside diphosphate kinase from mimivirus:
        a peculiar affinity for deoxypyrimidine nucleotides. J Bioenerg Biomembr [Internet].
        2006 Aug [cited 2022 Aug 21];38(3–4):247–54. Available from:
        https://pubmed.ncbi.nlm.nih.gov/16957983/

28.   Dzeja P, Terzic A. Adenylate kinase and AMP signaling networks: metabolic
        monitoring, signal communication and body energy sensing. Int J Mol Sci [Internet].
        2009 Apr [cited 2022 Aug 21];10(4):1729–72. Available from:
        https://pubmed.ncbi.nlm.nih.gov/19468337/

29.   Lu Q, Inouye M. Adenylate kinase complements nucleoside diphosphate kinase
        deficiency in nucleotide metabolism. Proc Natl Acad Sci U S A [Internet]. 1996 Jun 11
        [cited 2022 Aug 21];93(12):5720–5. Available from:
        https://pubmed.ncbi.nlm.nih.gov/8650159/

30.   Bernard MA, Ray NB, Olcott MC, Hendricks SP, Mathews CK. Metabolic functions of
        microbial nucleoside diphosphate kinases. J Bioenerg Biomembr [Internet]. 2000 [cited
        2022 Aug 21];32(3):259–67. Available from:
        https://pubmed.ncbi.nlm.nih.gov/11768309/

31.   Willemoës M, Kilstrup M. Nucleoside triphosphate synthesis catalysed by adenylate
        kinase is ADP dependent. Arch Biochem Biophys [Internet]. 2005 Dec 15 [cited 2022
        Aug 21];444(2):195–9. Available from: https://pubmed.ncbi.nlm.nih.gov/16297370/

32.   Müller CW, Schulz GE. Structure of the complex between adenylate kinase from
        Escherichia coli and the inhibitor Ap5A refined at 1.9 A resolution. A model for a
        catalytic transition state. J Mol Biol [Internet]. 1992 Mar 5 [cited 2022 Aug
        21];224(1):159–77. Available from: https://pubmed.ncbi.nlm.nih.gov/1548697/

33.   Thymark M, Johansson E, Larsen S, Willemoës M. Mutational analysis of the
        nucleotide binding site of Escherichia coli dCTP deaminase. Arch Biochem Biophys.
        2008 Feb;470(1):20–6.

34.   Johansson E, Thymark M, Bynck JH, Fanø M, Larsen S, Willemoës M. Regulation of
        dCTP deaminase from Escherichia coli by nonallosteric dTTP binding to an inactive
        form of the enzyme. FEBS J. 2007 Aug;274(16):4188–98.

35.   Finer-Moore JS, Santi D V., Stroud RM. Lessons and conclusions from dissecting the
        mechanism of a bisubstrate enzyme: thymidylate synthase mutagenesis, function, and
        structure. Biochemistry [Internet]. 2003 Jan 21 [cited 2022 Aug 21];42(2):248–56.
        Available from: https://pubmed.ncbi.nlm.nih.gov/12525151/

36.   Montfort WR, Perry KM, Fauman EB, Finer-Moore JS, Maley GF, Hardy L, et al.
        Structure, multiple site binding, and segmental accommodation in thymidylate synthase
        on binding dUMP and an anti-folate. Biochemistry [Internet]. 1990 Jan 1 [cited 2022
        Aug 21];29(30):6964–77. Available from: https://pubmed.ncbi.nlm.nih.gov/2223754/

37.   Arvizu-Flores AA, Sugich-Miranda R, Arreola R, Garcia-Orozco KD, Velazquez-
        Contreras EF, Montfort WR, et al. Role of an invariant lysine residue in folate binding
        on Escherichia coli thymidylate synthase: calorimetric and crystallographic analysis of
        the K48Q mutant. Int J Biochem Cell Biol [Internet]. 2008 [cited 2022 Aug

21];40(10):2206–17. Available from: https://pubmed.ncbi.nlm.nih.gov/18403248/

38.   Nelson DJ, Carter CE. Purification and Characterization of Thymidine 5'-Monophosphate Kinase from Escherichia coli B*. J Biol Chem. 1969;244(19):5254–62.

39.   Munier-Lehmann H, Chaffotte A, Pochet S, Labesse G. Thymidylate kinase of Mycobacterium tuberculosis: a chimera sharing properties common to eukaryotic and bacterial enzymes. Protein Sci [Internet]. 2001 Jun [cited 2022 Aug 21];10(6):1195–205. Available from: https://pubmed.ncbi.nlm.nih.gov/11369858/

40.   Reynes JP, Tiraby M, Baron M, Drocourt D, Tiraby G. Escherichia coli thymidylate kinase: molecular cloning, nucleotide sequence, and genetic organization of the corresponding tmk locus. J Bacteriol [Internet]. 1996 [cited 2022 Aug 21];178(10):2804–12. Available from: https://pubmed.ncbi.nlm.nih.gov/8631667/

41.   Daws TD, Fuchs JA. Isolation and characterization of an Escherichia coli mutant deficient in dTMP kinase activity. J Bacteriol [Internet]. 1984 [cited 2022 Aug 21];157(2):440–4. Available from: https://pubmed.ncbi.nlm.nih.gov/6319360/

42.   Batada NN, Westover KD, Bushnell DA, Levitt M, Kornberg RD. Diffusion of nucleoside triphosphates and role of the entry site to the RNA polymerase II active center. Proc Natl Acad Sci U S A. 2004 Dec 14;101(50):17361–4.

43.   Milo R, Jorgensen P, Moran U, Weber G, Springer M. BioNumbers--the database of key numbers in molecular and cell biology. Nucleic Acids Res [Internet]. 2010 Oct 23 [cited 2022 Aug 21];38(Database issue). Available from: https://pubmed.ncbi.nlm.nih.gov/19854939/

44.   Moen LK, Howell ML, Lasser GW, Mathews CK. T4 phage deoxyribonucleoside triphosphate synthetase: purification of an enzyme complex and identification of gene products required for integrity. J Mol Recognit [Internet]. 1988 [cited 2022 Aug 21];1(1):48–57. Available from: https://pubmed.ncbi.nlm.nih.gov/3078839/

45.   Shen R, Olcott MC, Kim JH, Rajagopal I, Mathews CK. Escherichia coli nucleoside diphosphate kinase interactions with T4 phage proteins of deoxyribonucleotide synthesis and possible regulatory functions. J Biol Chem [Internet]. 2004 Jul 30 [cited 2022 Aug 21];279(31):32225–32. Available from: https://pubmed.ncbi.nlm.nih.gov/15169771/

46.   Shen R, Wheeler LJ, Mathews CK. Molecular interactions involving Escherichia coli nucleoside diphosphate kinase. J Bioenerg Biomembr [Internet]. 2006 Aug [cited 2022 Aug 21];38(3–4):255–9. Available from: https://pubmed.ncbi.nlm.nih.gov/16957984/

47.   Kim J, Wheeler LJ, Shen R, Mathews CK. Protein-DNA interactions in the T4 dNTP synthetase complex dependent on gene 32 single-stranded DNA-binding protein. Mol Microbiol. 2005 Mar;55(5):1502–14.

48.   Kim JH, Shen R, Olcott MC, Rajagopal I, Mathews CK. Adenylate kinase of Escherichia coli, a component of the phage T4 dNTP synthetase complex. J Biol Chem. 2005 Aug 5;280(31):28221–9.

49.   Reddy GPV, Singh A, Stafford ME, Mathews CK. Enzyme associations in T4 phage DNA precursor synthesis. Proc Natl Acad Sci U S A [Internet]. 1977 [cited 2022 Aug

21];74(8):3152–6. Available from: https://pubmed.ncbi.nlm.nih.gov/198773/

50. Anderson DD, Woeller CF, Chiang EP, Shane B, Stover PJ. Serine hydroxymethyltransferase anchors de novo thymidylate synthesis pathway to nuclear lamina for DNA synthesis. J Biol Chem [Internet]. 2012 Mar 2 [cited 2022 Aug 21];287(10):7051–62. Available from: https://pubmed.ncbi.nlm.nih.gov/22235121/

51. Luzarowski M, Kosmacz M, Sokolowska E, Jasińska W, Willmitzer L, Veyel D, et al. Affinity purification with metabolomic and proteomic analysis unravels diverse roles of nucleoside diphosphate kinases. J Exp Bot [Internet]. 2017 Aug 22 [cited 2022 Aug 21];68(13):3487–99. Available from: https://pubmed.ncbi.nlm.nih.gov/28586477/

52. Dawes SS, Warner DF, Tsenova L, Timm J, McKinney JD, Kaplan G, et al. Ribonucleotide Reduction in Mycobacterium tuberculosis: Function and Expression of Genes Encoding Class Ib and Class II Ribonucleotide Reductases. Infect Immun [Internet]. 2003 Nov [cited 2022 Aug 21];71(11):6124. Available from: /pmc/articles/PMC219568/

53. Masalha M, Borovok I, Schreiber R, Aharonowitz Y, Cohen G. Analysis of transcription of the Staphylococcus aureus aerobic class Ib and anaerobic class III ribonucleotide reductase genes in response to oxygen. J Bacteriol [Internet]. 2001 [cited 2022 Aug 21];183(24):7260–72. Available from: https://pubmed.ncbi.nlm.nih.gov/11717286/

enzyme	catalysed reaction	reaction step	equation	parameter name	parameter value	parameter dimension	from literature or calculated	note	reference
adenylate kinase (amk)	dAMP phosphorylation	dAMP binding	AMK + dAMP = AMK.dAMP	Michaelis constant (Km)	1,7	mM	literature	-	(Holmes és Singer, 1973)
adenylate kinase (amk)	(d)AMP phosphorylation	ATP binding	AMK + ATP = AMK.ATP	Michaelis constant (Km)	0,38	mM	literature	-	(Holmes és Singer, 1973)
adenylate kinase (amk)	dAMP phosphorylation	dAMP phosphorylation by ATP	AMK.ADP.dADP = AMK.ATP.dAMP	Vmax	44600	mol substrate/ min/ mol enzyme	literature	-	(Holmes és Singer, 1973)
adenylate kinase (amk)	dAMP phosphorylation	dAMP phosphorylation by ATP reverse	AMK.ADP.dADP = AMK.ATP.dAMP	kcat	600	1/s	calculated	Based on (Bernard, 2000), calculated using reaction K'	-
adenylate kinase (amk)	dAMP phosphorylation	dADP binding	AMK + dADP = AMK.dADP	Michaelis constant (Km)	0,92	mM	literature	-	(Bernard és mtsai., 2000)
adenylate kinase (amk)	(d)AMP phosphorylation	ADP binding	AMK + ADP = AMK.ADP	Michaelis constant (Km)	0,09	mM	literature	-	(Holmes és Singer, 1973)
adenylate kinase (amk)	(d)AMP phosphorylation	dATP binding	AMK + dATP = AMK.dATP	Michaelis constant (Km)	0,25	mM	literature	-	(Holmes és Singer, 1973)
adenylate kinase (amk)	(d)AMP phosphorylation	dAMP phosphorylation by dATP	AMK.dADP.dADP = AMK.dATP.dAMP	Vmax	44600	mol substrate/ min/ mol enzyme	calculated	dAMP-ATP data used from (Bernard, 2000)	-

adenylate kinase (amk)	(d)AMP phosphorylation	dAMP phosphorylation by dATP reverse	AMK.dADP.dADP = AMK.dATP.dAMP	kcat	670	1/s	calculated	Based on (Bernard, 2000), calculated using reaction K'	-
adenylate kinase (amk)	(d)AMP phosphorylation	AMP binding	AMK + AMP = AMK.AMP	Michaelis constant (Km)	0,14	mM	literature	-	(Holmes és Singer, 1973)
adenylate kinase (amk)	(d)AMP phosphorylation	AMP phosphorylation by ATP	AMK.ADP.ADP = AMK.ATP.AMP	Vmax	16500	mol substrate/ min/ mol enzyme	literature	-	(Holmes és Singer, 1973)
adenylate kinase (amk)	(d)AMP phosphorylation	AMP phosphorylation by ATP reverse	AMK.ADP.ADP = AMK.ATP.AMP	Vmax	15800	mol substrate/ min/ mol enzyme	literature	-	(Holmes és Singer, 1973)
adenylate kinase (amk)	dATP production	dADP phosphorylation	AMK.ADP.dADP = AMK.AMP.dATP	kcat	6	1/s	literature	-	(Bernard és mtsai., 2000)
adenylate kinase (amk)		dADP phosphorylation reverse	AMK.ADP.dADP = AMK.AMP.dATP	kcat	7	1/s	calculated	Based on (Bernard, 2000), calculated using reaction K'	-
adenylate kinase (amk)	dGTP production	dGDP binding	AMK + dGDP = AMK.dGDP	Michaelis constant (Km)	0,497	µM	literature	-	(Bernard és mtsai., 2000)
adenylate kinase (amk)	dGTP production	dGTP phosphorylation by ADP	AMK.ADP.dGDP = AMK.AMP.dGTP	kcat	7	1/s	calculated	Based on (Bernard, 2000), calculated using reaction K'	-
adenylate kinase (amk)	dGTP production	dGTP phosphorylation by ADP reverse	AMK.ADP.dGDP = AMK.AMP.dGTP	kcat	4,1	1/s	literature	-	(Bernard és mtsai., 2000)
adenylate kinase (amk)	dGTP production	dGTP binding	AMK + dGTP = AMK.dGTP	Michaelis constant (Km)	3570	µM	calculated	calculated from other NTP and NDP affinities	-
adenylate kinase (amk)	dGTP production	dGTP phosphorylation by dADP	AMK.dADP.dGDP = AMK.dAMP.dGTP	kcat	9	1/s	calculated	Based on (Bernard, 2000), calculated using reaction K'	-

adenylate kinase (amk)	dGTP production	dGTP phosphorylation by dADP reverse	AMK.dADP.dGDP = AMK.dAMP.dGTP	kcat	4	1/s	calculated	(Bernard, 2000), dGDP-ADP data used	(Bernard *és mtsai.*, 2000)
adenylate kinase (amk)	dCTP production	dCDP binding	AMK + dCDP = AMK.dCDP	Michaelis constant (Km)	2180	µM	literature	-	(Bernard *és mtsai.*, 2000)
adenylate kinase (amk)	dCTP production	dCDP phosphorylation by ADP	AMK.ADP.dCDP = AMK.AMP.dCTP	kcat	1	1/s	calculated	Based on (Bernard, 2000), calculated using reaction K'	-
adenylate kinase (amk)	dCTP production	dCDP phosphorylation by ADP reverse	AMK.ADP.dCDP = AMK.AMP.dCTP	kcat	5	1/s	literature	-	(Bernard *és mtsai.*, 2000)
adenylate kinase (amk)	dCTP production	dCTP binding	AMK + dCTP = AMK.dCTP	Michaelis constant (Km)	1250	µM	calculated	calculated from other NTP and NDP affinities	-
adenylate kinase (amk)	dCTP production	dCDP phosphorylation by dADP	AMK.dADP.dCDP = AMK.dAMP.dCTP	kcat	1	1/s	calculated	Based on (Bernard, 2000), calculated using reaction K'	-
adenylate kinase (amk)	dCTP production	dCDP phosphorylation by dADP reverse	AMK.dADP.dCDP = AMK.dAMP.dCTP	kcat	5	1/s	calculated	(Bernard, 2000), dCDP-ADP data used	-
adenylate kinase (amk)	dTTP production	dTDP binding	AMK + dTDP = AMK.dTDP	Michaelis constant (Km)	458	µM	literature	-	(Bernard *és mtsai.*, 2000)
adenylate kinase (amk)	dTTP production	dTDP phosphorylation by ADP	AMK.ADP.dTDP = AMK.AMP.dTTP	kcat	3	1/s	calculated	Based on (Bernard, 2000), calculated using reaction K'	-
adenylate kinase (amk)	dTTP production	dTDP phosphorylation by ADP reverse	AMK.ADP.dTDP = AMK.AMP.dTTP	kcat	4	1/s	literature	-	(Bernard *és mtsai.*, 2000)
adenylate kinase (amk)	dTTP production	dTTP binding	AMK.dTTP = AMK + dTTP	Michaelis constant (Km)	1562	µM	calculated	calculated from other NTP and NDP affinities	-
adenylate kinase (amk)	dTTP production	dTDP phosphorylation by dADP	AMK.dADP.dTDP = AMK.dAMP.dTTP	kcat	4	1/s	calculated	Based on (Bernard, 2000), calculated using reaction K'	-

Enzyme	Process	Reaction description	Reaction	Parameter	Value	Unit	Source	Notes	Reference
adenylate kinase (amk)	dTTP production	dTDP phosphorylation by dADP reverse	AMK.dADP.dTDP = AMK.dAMP.dTTP	kcat	4	1/s	calculated	(Bernard, 2000), dTDP-ADP data used	-
guanylate kinase (gmk)	(d)GDP phosphorylation	ATP binding	GMK + ATP = GMK.ATP	Michaelis constant (Km)	63	µM	literature	-	(Hible *és mtsai.* , 2006)
guanylate kinase (gmk)	(d)GDP phosphorylation	dGMP binding	GMK + dGMP = GMK.dGMP	Michaelis constant (Km)	0,185	µM	calculated	calculated from literature data (5x the Km of GMP)	(Oeschger, 1978)
guanylate kinase (gmk)	(d)GDP phosphorylation	dGMP phosphorylation by ATP	GMK.dGMP.ATP = GMK.dGDP.ADP	kcat	188	1/s	calculated	Based on (Hibble, 2006), calculated using reaction K'	-
guanylate kinase (gmk)	(d)GDP phosphorylation	dGDP reverse reaction by ADP	GMK.dGMP.ATP = GMK.dGDP.ADP	kcat	55	1/s	calculated	Based on (Hibble, 2006), calculated using reaction K'	-
guanylate kinase (gmk)	(d)GDP phosphorylation	dGDP binding	GMK + dGDP = GMK.dGDP	Michaelis constant (Km)	0,17	µM	calculated	calculated from other NTP and NDP affinities	-
guanylate kinase (gmk)	(d)GDP phosphorylation	ADP binding	GMK + ADP = GMK.ADP	Michaelis constant (Km)	23	µM	literature	-	(Hible *és mtsai.* , 2006)
guanylate kinase (gmk)	(d)GDP phosphorylation	dATP binding	GMK + dATP = GMK.dATP	Michaelis constant (Km)	0,144	µM	calculated	calculated from other NTP and NDP affinities	-
guanylate kinase (gmk)	(d)GDP phosphorylation	dGMP phosphorylation by dATP	GMK.dGMP.dATP = GMK.dGDP.dADP	kcat	188	1/s	calculated	Based on (Hibble, 2006), calculated using reaction K'	-
guanylate kinase (gmk)	(d)GDP phosphorylation	dGDP reverse reaction by dADP	GMK.dGMP.dATP = GMK.dGDP.dADP	kcat	55	1/s	calculated	Based on (Hibble, 2006), calculated using reaction K'	-
guanylate kinase (gmk)	(d)GDP phosphorylation	dADP binding	GMK + dADP = GMK.dADP	Michaelis constant (Km)	53	µM	calculated	calculated from other NTP and NDP affinities	-
guanylate kinase (gmk)	(d)GDP phosphorylation	GMP binding	GMK + GMP = GMK.GMP	Michaelis constant (Km)	37	µM	literature	-	(Hible *és mtsai.* , 2006)

Enzyme	Process	Reaction	Equation	Parameter	Value	Unit	Source	Note	Reference
guanylate kinase (gmk)	(d)GDP phosphorylation	GMP phosphorylation by ATP	GMK.GMP.ATP = GMK.GDP.ADP	kcat	188	1/s	calculated	-	(Hible és mtsai. , 2006)
guanylate kinase (gmk)	(d)GDP phosphorylation	GDP reverse reaction by ATP	GMK.GMP.ATP = GMK.GDP.ADP	kcat	55	1/s	literature	-	(Hible és mtsai. , 2006)
guanylate kinase (gmk)	(d)GDP phosphorylation	GMP phosphorylation by dATP	GMK.GMP.dATP = GMK.GDP.dADP	kcat	188	1/s	calculated	Based on (Hibble, 2006), calculated using reaction K'	-
guanylate kinase (gmk)	(d)GDP phosphorylation	GDP reverse reaction by dATP	GMK.GMP.dATP = GMK.GDP.dADP	kcat	55	1/s	calculated	Based on (Hibble, 2006), calculated using reaction K'	-
guanylate kinase (gmk)	(d)GDP phosphorylation	GDP binding	GMK + GDP = GMK.GDP	Michaelis constant (Km)	33	µM	literature	-	(Hible és mtsai. , 2006)
cytidylate kinase (cmk)	(d)CMP phosphorylation	ATP binding	CMK + ATP = CMK.ATP	Michaelis constant (Km)	0,038	mM	literature		(Bucurenci és mtsai. , 1996)
cytidylate kinase (cmk)	dCMP phosphorylation	dCMP binding	CMK + dCMP = CMK.dCMP	Michaelis constant (Km)	0,094	mM	literature		(Bucurenci és mtsai. , 1996)
cytidylate kinase (cmk)	dCMP phosphorylation	dCMP phosphorylation by ATP	CMK.dCMP.ATP = CMK.dCDP.ADP	specific activity	226	µmol/ mg*min	literature	average of measured parameters from literature	
cytidylate kinase (cmk)	dCMP phosphorylation by dATP	dCMP phosphorylation by dATP	CMK.dCMP.dATP = CMK.dCDP.dADP	specific activity	219	µmol/ mg*min	literature	average of measured parameters from literature	
cytidylate kinase (cmk)	dCMP phosphorylation by ATP	dCDP reverse reaction by ADP	CMK.dCMP.ATP = CMK.dCDP.ADP	kcat	202	1/s	calculated	calculated from K' calculated for reaction	-
cytidylate kinase (cmk)	dCMP phosphorylation by dATP	dCDP reverse reaction by dADP	CMK.dCMP.dATP = CMK.dCDP.dADP	kcat	222	1/s	calculated	calculated from K' calculated for reaction	-
cytidylate kinase (cmk)	dCMP phosphorylation by ATP	dCDP binding	CMK + dCDP = CMK.dCDP	Michaelis constant (Km)	0,14	mM	calculated	calculated from other Km parameters	-

cytidylate kinase (cmk)	(d)CMP phosphorylation	ADP binding	CMK + ADP = CMK.ADP	Michaelis constant (Km)	0,025	mM	literature		(Bucurenci *és mtsai.*, 1996)
cytidylate kinase (cmk)	(d)CMP phosphorylation	dATP binding	CMK + dATP = CMK.dATP	Michaelis constant (Km)	0,087	mM	literature		(Bucurenci *és mtsai.*, 1996)
cytidylate kinase (cmk)	(d)CMP phosphorylation	dADP binding	CMK + dADP = CMK.dADP	Michaelis constant (Km)	0,067	mM	calculated	calculated from other Km parameters	-
cytidylate kinase (cmk)	CMP phosphorylation	CMP binding	CMK + CMP = CMK.CMP	Michaelis constant (Km)	0,035	mM	literature		(Bucurenci *és mtsai.*, 1996)
cytidylate kinase (cmk)	CMP phosphorylation by ATP	CMP phosphorylation by ATP	CMK.CMP.ATP = CMK.CDP.ADP	specific activity	220	µmol/mg*min	literature	average of measured parameters from literature	
cytidylate kinase (cmk)	CMP phosphorylation by dATP	CMP phosphorylation by dATP	CMK.CMP.dATP = CMK.CDP.dADP	specific activity	212	µmol/mg*min	literature	average of measured parameters from literature	
cytidylate kinase (cmk)	CMP phosphorylation by ATP	CDP reverse reaction by ATP	CMK.CMP.ATP = CMK.CDP.ADP	specific activity	410	µmol/mg*min	literature		(Bucurenci *és mtsai.*, 1996)
cytidylate kinase (cmk)	CMP phosphorylation by dATP	CDP reverse reaction by dATP	CMK.CMP.dATP = CMK.CDP.dADP	kcat	214	1/s	calculated	calculated from K' calculated for reaction	-
cytidylate kinase (cmk)	CMP phosphorylation	CDP binding	CMK + CDP = CMK.CDP	Michaelis constant (Km)	0,052	mM	literature		(Bucurenci *és mtsai.*, 1996)
thymidylate kinase (tmk)	dTMP phosphorylation by ATP	ATP binding	TMK + dATP = TMK.dATP	Michaelis constant (Km)	40	µM	literature		(Munier-Lehmann *és mtsai.*, 2001)
thymidylate kinase (tmk)	dTMP phosphorylation by ATP	dTMP binding	TMK + dTMP = TMK.dTMP	Michaelis constant (Km)	15	µM	literature		(Munier-Lehmann *és mtsai.*, 2001)
thymidylate kinase (tmk)	dTMP phosphorylation by ATP	dTMP phosphorylation by ATP	TMK.dTMP.ATP = TMK.dTDP.ADP	kcat	10,5	1/s	literature		(Munier-Lehmann *és mtsai.*, 2001)

thymidylate kinase (tmk)	dTMP phosphorylation by ATP	dTMP phosphorylation by ATP reverse	TMK.dTMP.ATP = TMK.dTDP.ADP	kcat	5,4	1/s	calculated	Calculated from K' and Km data	-
thymidylate kinase (tmk)	dTMP phosphorylation by ATP	dTDP binding	TMK + dTDP = TMK.dTDP	Michaelis constant (Km)	18	µM	calculated	calculated from other NTP and NDP affinities	-
thymidylate kinase (tmk)	dTMP phosphorylation by ATP	ADP binding	TMK + ADP = TMK.ADP	Michaelis constant (Km)	24	µM	calculated	calculated from other NTP and NDP affinities	-
thymidylate kinase (tmk)	dTMP phosphorylation by dATP	dATP binding	TMK + dATP = TMK.dATP	Michaelis constant (Km)	53	µM	calculated from literature	Calculated from (Munier-Lehmann, 2001.) 76% of ATP	-
thymidylate kinase (tmk)	dTMP phosphorylation by dATP	dTMP phosphorylation by dATP	TMK.dTMP.dATP = TMK.dTDP.dADP	kcat	10,5	1/s	calculated from literature	Based on (Munier-Lehmann, 2001.), calculated using reaction K'	-
thymidylate kinase (tmk)	dTMP phosphorylation by dATP	dTMP phosphorylation by dATP reverse	TMK.dTMP.dATP = TMK.dTDP.dADP	kcat	5,4	1/s	calculated from literature	Based on (Munier-Lehmann, 2001.), calculated using reaction K'	-
thymidylate kinase (tmk)	dTMP phosphorylation by dATP	dADP binding	TMK + dADP = TMK.dADP	Michaelis constant (Km)	32	µM	calculated		-
thymidylate kinase (tmk)		dUDP binding	TMK + dUDP = TMK.dUDP	Michaelis constant (Km)	2500	µM	literature		(Tourneux *és mtsai.*, 1998)
thymidylate kinase (tmk)	dTMP phosphorylation by dGTP	dGTP binding	TMK + dGTP = TMK.dGTP	Michaelis constant (Km)	114	µM	calculated from literature	Calculated from (Munier-Lehmann, 2001.) 35% of ATP	-
thymidylate kinase (tmk)	dTMP phosphorylation by dGTP	dTMP phosphorylation by dGTP	TMK.dTMP.dGTP = TMK.dTDP.dGDP	kcat	10,5	1/s	calculated	Based on (Munier-Lehmann, 2001.)	-
thymidylate kinase (tmk)	dTMP phosphorylation by dGTP	dTMP phosphorylation by dGTP reverse	TMK.dTMP.dGTP = TMK.dTDP.dGDP	kcat	16,4	1/s	calculated	Based on (Munier-Lehmann, 2001.), calculated using reaction K'	-

thymidylate kinase (tmk)	dTMP phosphorylation by dGTP	dGDP binding	TMK + dGDP = TMK.dGDP	Michaelis constant (Km)	211	μM	calculated	calculated from other NTP and NDP affinities	-
thymidylate kinase (tmk)	dTMP phosphorylation by CTP	CTP binding	TMK + CTP = TMK.CTP	Michaelis constant (Km)	167	μM	calculated from literature	Calculated from (Munier-Lehmann, 2001.) 24% of ATP	-
thymidylate kinase (tmk)	dTMP phosphorylation by CTP	dTMP phosphorylation by CTP	TMK.dTMP.CTP = TMK.dTDP.CDP	kcat	10,5	1/s	calculated	Based on (Munier-Lehmann, 2001.)	-
thymidylate kinase (tmk)	dTMP phosphorylation by CTP	dTMP phosphorylation by CTP reverse	TMK.dTMP.CTP = TMK.dTDP.CDP	kcat	5,4	1/s	calculated	Based on (Munier-Lehmann, 2001.), calculated using reaction K'	-
thymidylate kinase (tmk)	dTMP phosphorylation by CTP	CDP binding	TMK + CTP = TMK.CTP	Michaelis constant (Km)	100	μM	calculated	calculated from other NTP and NDP affinities	-
nucleotide diphosphate kinase (ndk)	NDK phosphorylation by ATP	ATP binding	NDK + ATP = NDK.ATP	Michaelis constant (Km)	22	mM	literature (S.cerevisiae)		
nucleotide diphosphate kinase (ndk	NDK phosphorylation by ATP	Phosphorylation by ATP	NDK.ATP = NDK-P.ADP	kcat	130	mM/min	literature (S.cerevisiae)		
nucleotide diphosphate kinase (ndk	NDK phosphorylation by ATP	Phosphorylation by ATP reverse	NDK.ATP = NDK-P.ADP	kcat	170	mM/min	literature (S.cerevisiae)		
nucleotide diphosphate kinase (ndk	NDK phosphorylation by ATP	ADP binding	NDK-P.ADP = NDK-P + ADP	Michaelis constant (Km)	0,03	mM	literature (S.cerevisiae)		
nucleotide diphosphate kinase (ndk	NDK phosphorylation by GTP	GTP binding	NDK + GTP = NDK.GTP	Michaelis constant (Km)	0,15	mM	literature (S.cerevisiae)		
nucleotide diphosphate kinase (ndk	NDK phosphorylation by GTP	Phosphorylation by GTP	NDK.GTP = NDK-P.GDP	kcat	268	mM/min	literature (S.cerevisiae)	calculated from other NTP and NDP affinities	

nucleotide diphosphate kinase (ndk	NDK phosphorylation by GTP	Phosphorylation by GTP reverse	NDK.GTP = NDK-P.GDP	kcat	350	mM/min	literature (S.cerevisiae)	
nucleotide diphosphate kinase (ndk	NDK phosphorylation by GTP	GDP binding	NDK-P.GDP = NDK-P + GDP	Michaelis constant (Km)	1,5	mM	literature (S.cerevisiae)	calculated from other NTP and NDP affinities
nucleotide diphosphate kinase (ndk	NDK phosphorylation by CTP	CTP binding	NDK + CTP = NDK.CTP	Michaelis constant (Km)	0,1	mM	literature (S.cerevisiae)	
nucleotide diphosphate kinase (ndk	NDK phosphorylation by CTP	Phosphorylation by CTP	NDK.CTP = NDK-P.CDP	kcat	220	mM/min	literature (S.cerevisiae)	
nucleotide diphosphate kinase (ndk	NDK phosphorylation by CTP	Phosphorylation by CTP reverse	NDK.CTP = NDK-P.CDP	kcat	83	mM/min	literature (S.cerevisiae)	
nucleotide diphosphate kinase (ndk	NDK phosphorylation by CTP	CDP binding	NDK-P.CDP = NDK-P + CDP	Michaelis constant (Km)	0,3	mM	literature (S.cerevisiae)	
nucleotide diphosphate kinase (ndk	NDK phosphorylation by UTP	UTP binding	NDK + UTP = NDK.UTP	Michaelis constant (Km)	0,14	mM	literature (S.cerevisiae)	
nucleotide diphosphate kinase (ndk	NDK phosphorylation by UTP	Phosphorylation by UTP	NDK.UTP = NDK-P.UDP	kcat	400	mM/min	literature (S.cerevisiae)	
nucleotide diphosphate kinase (ndk	NDK phosphorylation by UTP	Phosphorylation by UTP reverse	NDK.UTP = NDK-P.UDP	kcat	75	mM/min	literature (S.cerevisiae)	
nucleotide diphosphate kinase (ndk	NDK phosphorylation by UTP	UDP binding	NDK-P.UDP = NDK-P + UDP	Michaelis constant (Km)	0,69	mM	literature (S.cerevisiae)	
nucleotide diphosphate kinase (ndk	NDK phosphorylation by dATP	dATP binding	NDK + dATP = NDK.dATP	Michaelis constant (Km)	0,13	mM	literature (S.cerevisiae)	calculated from other NTP and NDP affinities

nucleotide diphosphate kinase (ndk	NDK phosphorylation by dATP	Phosphorylation by dATP	NDK + dATP = NDK.dATP	kcat	139	mM/min	literature (S.cerevisiae)	calculated from other NTP and NDP affinities
nucleotide diphosphate kinase (ndk	NDK phosphorylation by dATP	Phosphorylation by dATP reverse	NDK + dATP = NDK.dATP	kcat	40	mM/min	literature (S.cerevisiae)	
nucleotide diphosphate kinase (ndk	NDK phosphorylation by dATP	dADP binding	NDK + dATP = NDK.dATP	Michaelis constant (Km)	0,5	mM	literature (S.cerevisiae)	calculated from other NTP and NDP affinities
nucleotide diphosphate kinase (ndk	NDK phosphorylation by dCTP	dCTP binding	NDK + dCTP = NDK.dCTP	Michaelis constant (Km)	0,17	mM	literature (S.cerevisiae)	
nucleotide diphosphate kinase (ndk	NDK phosphorylation by dCTP	Phosphorylation by dCTP	NDK-P.dCDP = NDK.dCTP	kcat	380	mM/min	literature (S.cerevisiae)	
nucleotide diphosphate kinase (ndk	NDK phosphorylation by dCTP	Phosphorylation by dCTP reverse	NDK-P.dCDP = NDK.dCTP	kcat	110	mM/min	literature (S.cerevisiae)	
nucleotide diphosphate kinase (ndk	NDK phosphorylation by dCTP	dCDP binding	NDK-P.dCDP = NDK-P + dCDP	Michaelis constant (Km)	0,4	mM	literature (S.cerevisiae)	
nucleotide diphosphate kinase (ndk	NDK phosphorylation by dGTP	dGTP binding	NDK + dGTP = NDK.dGTP	Michaelis constant (Km)	0,02	mM	literature (S.cerevisiae)	
nucleotide diphosphate kinase (ndk	NDK phosphorylation by dGTP	Phosphorylation by dGTP	NDK-P.dGDP = NDK.dGTP	kcat	132	mM/min	literature (S.cerevisiae)	
nucleotide diphosphate kinase (ndk	NDK phosphorylation by dGTP	Phosphorylation by dGTP reverse	NDK-P.dGDP = NDK.dGTP	kcat	38	mM/min	literature (S.cerevisiae)	
nucleotide diphosphate kinase (ndk	NDK phosphorylation by dGTP	dGDP binding	NDK-P.dGDP = NDK-P + dGDP	Michaelis constant (Km)	0,22	mM	literature (S.cerevisiae)	

(Jeudy, Claverie és Abergel, 2006)

nucleotide diphosphate kinase (ndk	NDK phosphorylation by dTTP	dTTP binding	NDK + dTTP = NDK.dTTP	Michaelis constant (Km)	0,11	mM	literature (S.cerevisiae)	
nucleotide diphosphate kinase (ndk	NDK phosphorylation by dTTP	Phosphorylation by dTTP	NDK-P.dTDP = NDK.dTTP	kcat	330	mM/min	literature (S.cerevisiae)	
nucleotide diphosphate kinase (ndk	NDK phosphorylation by dTTP	Phosphorylation by dTTP reverse	NDK-P.dTDP = NDK.dTTP	kcat	105	mM/min	literature (S.cerevisiae)	
nucleotide diphosphate kinase (ndk	NDK phosphorylation by dTTP	dTDP binding	NDK-P.dTDP = NDK-P + dTDP	Michaelis constant (Km)	0,37	mM	literature (S.cerevisiae)	
nucleotide diphosphate kinase (ndk	NDK phosphorylation by dUTP	dUTP binding	NDK + dUTP = NDK.dUTP	Michaelis constant (Km)	0,13	mM	literature (S.cerevisiae)	
nucleotide diphosphate kinase (ndk	NDK phosphorylation by dUTP	Phosphorylation by dUTP	NDK-P.dUDP = NDK.dUTP	kcat	8600	mM/min	literature (S.cerevisiae)	
nucleotide diphosphate kinase (ndk	NDK phosphorylation by dUTP	Phosphorylation by dUTP reverse	NDK-P.dUDP = NDK.dUTP	kcat	90	mM/min	literature (S.cerevisiae)	
nucleotide diphosphate kinase (ndk	NDK phosphorylation by dUTP	dUDP binding	NDK-P.dUDP = NDK-P + dUDP	Michaelis constant (Km)	0,53	mM	literature (S.cerevisiae)	
Thymidylate synthase (thyA)	dTMP synthesys	dUMP binding	ThyA + dUMP = ThyA.dUMP	Michaelis constant (Km)	4,1	µM	literature	-	
Thymidylate synthase (thyA)	dTMP synthesys	mTHF binding	ThyA + mTHF = ThyA.mTHF	Michaelis constant (Km)	13,6	µM	literature	-	(Reyes *és mtsai.* , 1998)
Thymidylate synthase (thyA)	dTMP synthesys	dTMP synthesys	ThyA.dUMP.mTHF -> ThyA + dTMP + DHF	kcat	8,8	1/s	literature	-	

Enzyme	Process	Step	Reaction	Parameter	Value	Unit	Source	Notes	Reference
dUTPase (dut)	dUMP formation from dUTP	dUTP binding	dUTP + DUT = dUTP.DUT	Michaelis constant (Km)	0.5	μM	literature	-	(Barabás és mtsai. , 2004)
dUTPase (dut)	dUMP formation from dUTP	dUMP formation	DUT.dUTP -> DUT + dUMP	kcat	11	1/s	literature	-	
dCTP deaminase (dcd)	dCTP deamination to dUTP	dCTP binding	DCD + dCTP = DCD.dCTP	S0,5	66	μM	literature	The addition of 100 μM dTTP increased the S0.5 to values of 168 ± 8 μM	(Johansson és mtsai. , 2007; Thymark és mtsai. , 2008)
dCTP deaminase (dcd)	dCTP deamination to dUTP	dUTP formation	DCD.dCTP -> dUTP	kcat	1,24	1/s	literature		
dCTP deaminase (dcd)	dCTP deamination to dUTP	dUTP formation	DCD.dCTP -> dUTP	Hill coefficience	1,5		literature	The addition of 100 μM dTTP increased the Hill coefficient for dCTP to 3.3	
dCTP deaminase (dcd)	dCTP deamination to dUTP	dTTP binding	DCD + dTTP = Inc_DCD	Kd	35	μM	literature		
ribonucleotide reductase (rnr)	RNR complex formation	Rnr formation from alpha and beta subunits	RNRa + RNRb = RNR	affinity (Kd)	0,34-0,41	uM	literature data	affinity of the a2 and b2 subunits for each other is weak (~0.4 mM) in the absence of effectors, whereas the binding of a complementary substrate/specificity effector pair increases the affinity of the class Ia RNR subunits fivefold	(Hassan és mtsai. , 2008; Zimanyi és mtsai. , 2016)
ribonucleotide reductase (rnr)	RNR complex formation	Rnr activation via ATP binding	RNR + ATP = Act_RNR	Km	80	uM	literature		(Ormö és Sjöberg, 1990)
ribonucleotide reductase (rnr)		rnr inhibition via dATP binding	RNR + dATP = InAct_RNR	Km	0,43	uM	literature		(Ormö és Sjöberg, 1990)
ribonucleotide reductase (rnr)	dNDP production with dTTP activator	dTTP binding	Act_RNR + dTTP = Act_RNR.dTTP	Km	1,9	uM	literature		(Ormö és Sjöberg, 1990)

ribonucleotide reductase (rnr)	dCDP production with dTTP activator	CDP binding	Act_RNR.dTTP + CDP = Act_RNR.dTTP.CDP	Km	50	uM	literature		(Larson és Reichard, 1966)
ribonucleotide reductase (rnr)	dCDP production with dTTP activator	CDP reduction	Act_RNR.dTTP.CDP -> Act_RNR + dTTP + dCDP	specific activity	1950	nmol/min/ mg	calculated	measured to dATP activation	(Zimanyi és mtsai. , 2016)
ribonucleotide reductase (rnr)	dGDP production with dTTP activator	GDP binding	Act_RNR.dTTP + GDP = Act_RNR.dTTP.GDP	Km	25	uM	literature		(Ormö és Sjöberg, 1990)
ribonucleotide reductase (rnr)	dGDP production with dTTP activator	GDP reduction	Act_RNR.dGTP.GDP -> Act_RNR + dGTP + dGDP	specific activity	1530	nmol/min/ mg	calculated	measured to dTTP activation	(Zimanyi és mtsai. , 2016)
ribonucleotide reductase (rnr)	dADP production with dTTP activator	ADP binding	Act_RNR.dTTP + ADP = Act_RNR.dTTP.ADP	Km	30	uM	literature		(Larsson és Reichard, 1966)
ribonucleotide reductase (rnr)	dADP production with dTTP activator	ADP reduction	Act_RNR.dTTP.ADP -> Act_RNR + dTTP + dADP	specific activity	1200	nmol/min/ mg	calculated	measured to dGTP activation	(Zimanyi és mtsai. , 2016)
ribonucleotide reductase (rnr)	dUDP production with dTTP activator	UDP binding	Act_RNR.dTTP + UDP = Act_RNR.dTTP.UDP	Km	220	uM	literature		(Larson és Reichard, 1966)
ribonucleotide reductase (rnr)	dUDP production with dTTP activator	UDP reduction	Act_RNR.dTTP.UDP -> Act_RNR + dTTP + dUDP	specific activity	2600	nmol/min/ mg	calculated	measured to dATP activation	(Zimanyi és mtsai. , 2016)
ribonucleotide reductase (rnr)	dNDP production with dGTP activator	dGTP binding	Act_RNR + dGTP = Act_RNR.dGTP	Km	0,77	uM	literature		(Ormö és Sjöberg, 1990)
ribonucleotide reductase (rnr)	dADP production with dGTP activator	ADP binding	Act_RNR.dGTP + ADP = Act_RNR.dGTP.ADP	Km	30	uM	literature		(Larsson és Reichard, 1966)
ribonucleotide reductase (rnr)	dADP production with dGTP activator	ADP reduction	Act_RNR.dGTP.ADP -> Act_RNR + dGTP + dADP	specific activity	1200	nmol/min/ mg	calculated	measured to dGTP activation	(Zimanyi és mtsai. , 2016)
ribonucleotide reductase (rnr)	dNDP production with dATP activator	dATP binding	Act_RNR + dATP = Act_RNR.dATP	Km	6	uM	literature	allosteric activator	(Ormö és Sjöberg, 1990)
ribonucleotide reductase (rnr)	dCDP production with dATP activator	CDP binding	Act_RNR.dATP + CDP = Act_RNR.dATP.CDP	Km	50	uM	literature		(Larson és Reichard, 1966)
ribonucleotide reductase (rnr)	dCDP production with dATP activator	CDP reduction	Act_RNR.dATP.CDP -> dCDP + dATP + Act_RNR	specific activity	1950	nmol/min/ mg	literature	measured to dATP activation	(Zimanyi és mtsai. , 2016)
ribonucleotide reductase (rnr)	dUDP production with dATP activator	UDP binding	Act_RNR.dATP + UDP = Act_RNR.dATP.UDP	Km	220	uM	literature		(Larson és Reichard, 1966)

ribonucleotide reductase (rnr)	dUDP production with dATP activator	UDP reduction	Act_RNR.dATP.UDP -> dUDP + dATP + Act_RNR	specific activity	2600	nmol/mg/min	literature	measured to dATP activation	(Zimanyi *és mtsai.* , 2016)